water

MDPI

Article

Hydrogeochemistry and Water Quality Index for Groundwater Sustainability in the Komadugu-Yobe Basin, Sahel Region

Abdulrahman Shuaibu [1,2,*], Robert M. Kalin [1], Vernon Phoenix [1], Limbikani C. Banda [1] and Ibrahim Mohammed Lawal [1,3]

[1] Department of Civil and Environmental Engineering, University of Strathclyde, Glasgow G1 1XJ, UK; robert.kalin@strath.ac.uk (R.M.K.); vernon.phoenix@strath.ac.uk (V.P.); limbikani.chitsundi-banda@strath.ac.uk (L.C.B.); ibrahim.lawal@strath.ac.uk (I.M.L.)
[2] Department of Water Resource and Environmental Engineering, Ahmadu Bello University, Zaria 810107, Nigeria
[3] Department of Civil Engineering, Abubakar Tafawa Balewa University, Bauchi 740272, Nigeria
* Correspondence: abdulrahman.shuaibu@strath.ac.uk or shuaibua@abu.edu.ng; Tel.: +44-786-436-1870 or +234-803-802-8657

Abstract: The assessment of hydrochemical characteristics and groundwater quality is crucial for environmental sustainability in developing economies. This study employed hydrogeochemical analysis, geospatial analysis, and groundwater quality index to assess hydrogeochemical processes and quality of groundwater in the Komadugu-Yobe basin. The pH, total dissolved solids (TDS), and electrical conductivity (EC) were assessed in situ using a handheld portable electrical conductivity meter. The concentrations of the major cations (Na^+, Ca^{2+}, Mg^{2+}, and K^+), were analyzed using inductively coupled plasma optical emission spectroscopy (ICP-OES). The major anions (chloride, fluoride, sulfate, and nitrate) were analyzed via ion chromatography (IC). Total alkalinity and bicarbonate were measured in situ using a HACH digital alkalinity kit by the titrimetric method. Hydrochemical results indicate some physicochemical properties of the groundwater samples exceeded the maximum permissible limits as recommended by the World Health Organization guidelines for drinking water. Gibbs diagrams indicate rock–water interaction/rock weathering processes are the dominant mechanisms influencing the groundwater chemistry. Groundwater is predominantly Ca^{2+}-Mg^{2+}-HCO^-_3 water type, constituting 59% of the groundwater samples analyzed. The groundwater quality index (GWQI) depicted 63 and 27% of the groundwater samples as excellent and good water types for drinking purposes, respectively. This study further relates the interaction between geology, hydrochemical characteristics, and groundwater quality parameters. The results are essential to inform a sustainable management strategy and protection of groundwater resources.

Keywords: groundwater sustainability; geospatial analysis; water quality index; groundwater evolution; sustainable development goal 6 (SDG6)

Citation: Shuaibu, A.; Kalin, R.M.; Phoenix, V.; Banda, L.C.; Lawal, I.M. Hydrogeochemistry and Water Quality Index for Groundwater Sustainability in the Komadugu-Yobe Basin, Sahel Region. *Water* **2024**, *16*, 601. https://doi.org/10.3390/w16040601

Academic Editor: Cesar Andrade

Received: 19 January 2024
Revised: 9 February 2024
Accepted: 12 February 2024
Published: 18 February 2024

1. Introduction

Safe and sustainable freshwater resources are essential for socio-economic development and the well-being of humanity. Freshwater is vital for drinking, agriculture, sanitation, fisheries, hydropower generation, live stock farming, and recreation [1–4]. The main source water supply in most developing economies is groundwater from shallow wells [1,2,5–10]. The semi-arid to arid North-East region of Nigeria relies heavily on groundwater for various uses [11–14]. Consequently, it is crucial to ascertain the adequacy of the groundwater in terms of both quantity and quality for sustainable use and management in order to realize Sustainable Development Goal 6 (SDG6). However, impacts of anthropogenic activities pollute groundwater in Nigeria [15–17]. Various human activities such as excessive use of synthetic fertilizer and manure for irrigation purposes, dumping of solid wastes in rivers, leachate from dumpsites, septic tanks, and pit latrines pollute groundwater

in the Komadugu-Yobe basin [18]. Thus, the quality of the groundwater determines its usability [19,20].

Groundwater hydrogeochemical analysis provides an in-depth understanding of hydrochemical characteristics and the overall quality of groundwater [20–24]. The chemistry of groundwater is influenced by geological characteristics, the extent of chemical weathering of different rock formations, rock–water interaction, dissolution rates of various minerals, and the quality of the water that recharges the groundwater system [5,25–28]. Water quality is assessed and monitored using hydrogeochemical and statistical analysis, as well as the estimation of water quality indices [28,29]. The statistical analysis employed in water quality assessment elucidates the relationships between different water quality parameters. The water quality index (WQI) uses water quality parameters to represent the impact of geogenic and anthropogenic activities on overall water quality [4,23,29–33]. Many researchers employed the WQI in water quality studies because of its flexibility, adaptability, and simplicity in groundwater quality assessment and monitoring [2,22,24,34–37]. The WQI is also used to communicate water quality analysis results in a numerical format for easy communication and presentation to stakeholders, the general public, and government institutions [36–38].

A geographical information system (GIS) provides the spatial framework for evaluating water resource changes in space and time, such as water quality and quantity assessment, water pollution risks, and vulnerability mapping at both local and regional levels [8,30,39]. GISs are widely used for developing groundwater quality maps, which are essential for managing groundwater for various uses [2,4,33]. They are cost-efficient and transform large hydrochemical datasets into spatial information [8,39]. Geospatial techniques including inverse distance weight (IDW), Kriging, Spilain, and Cokriging interpolation algorithms in ArcGIS, are used to interpret the distribution of water quality parameters [4,33,34,38,39]. The IDW method is commonly employed as it uses a deterministic model approach [2,8,23,25,33,34,39,40].

Management of the water quality is needed for ecosystem health [7,22] and is critical for environmental quality management [35]. However, access to sufficient quantities of water of adequate quality for the people can be limited, particularly in arid and semi-arid parts of developing countries [22,41]. Assessment of the quality of available groundwater is essential for proper management and utilization. The quality of groundwater is influenced by various factors including subsurface hydrogeochemical processes, soil characteristics, seasonal variations, natural and anthropogenic activities, climate change, and groundwater recharge processes [19,34,42]. Moreover, municipal solid waste, industrial wastewater, and domestic wastewater impact groundwater quality [13,43]. Ganiyu et al. [7] indicated that WHO estimates 80% of human diseases resulted from poor water quality.

Previous studies within the Komadugu-Yobe basin did not focus on detailed geochemical assessments of the groundwater, though some local studies have been published [13,44–48]. To date, there have been no wide-ranging studies on groundwater quality assessment that integrate hydrogeochemical analysis, WQI, and GIS-based techniques. This study specifically addressed this knowledge gap. This study aims to provide information valuable to stakeholders, government institutions, and decision-makers involved in the sustainable management of groundwater resources in Nigeria and the wider Sahel region.

2. Materials and Methods

2.1. Study Area Setting

The Komadugu-Yobe basin is situated in the southwestern region of the greater Lake Chad basin. It covers a significant portion of the northwestern and northeastern parts of Nigeria within the Sahel region of Africa (Figure 1). The basin covers an approximate area of about 150,000 km^2, with an elevation of 294 m to 1750 m above the mean sea level. The Komadugu-Yobe and Komadugu-Gana sub-systems are the primary rivers within the basin. These rivers pass through the Hadejia Nguru wetland before ultimately draining into Lake Chad [49–51].

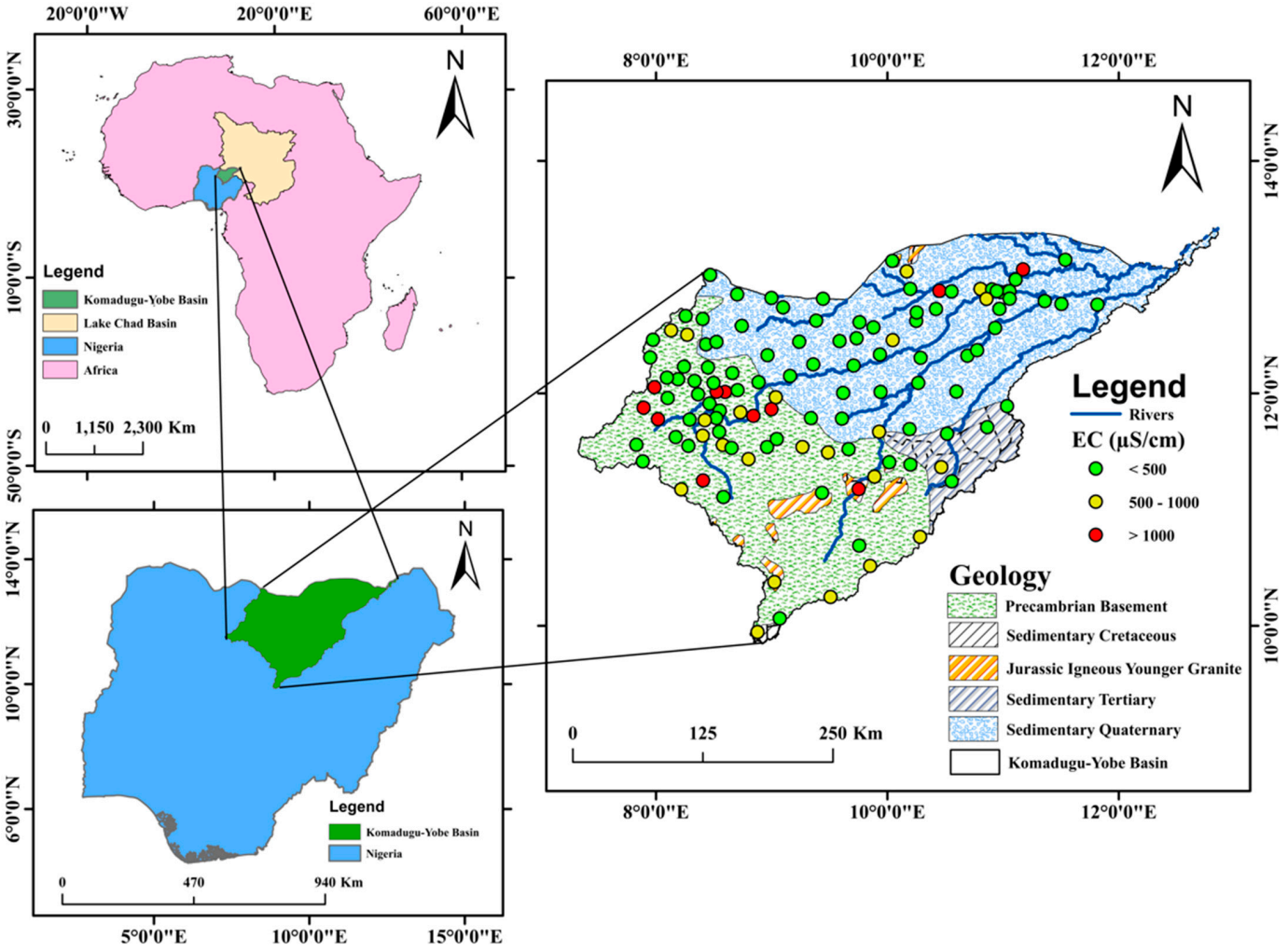

Figure 1. Groundwater sampling location, geology type, and electrical conductivity (EC) concentration in Komadugu-Yobe basin.

The basin has a semi-arid and arid climate characterized by severe drought and high rainfall variability. The wet season in the basin commences in May and extends through September and October, with the highest rainfall occurring in the month of August. The dry season spans from October to April [52]. The mean annual rainfall in the basin varies from a maximum of 1360 mm in Jos and 900 mm at Kano to a minimum of 600 mm and 400 mm around Hadejia and Nguru, respectively. The humidity in the basin is about 40%, and the annual evapotranspiration rate is 203 mm/year [49,52]. The basin has higher evaporation rates at the downstream section due to the high temperature. The annual maximum temperatures are recorded between March and April in the basin at 40 °C with a temperature of around 12 °C recorded in the months of December and January. The Komadugu-Yobe basin presently houses more than 20 million people. The wetlands in the Komadugu-Yobe basin provide the inhabitants residing in the basin with various economic activities such as fish production, pastoralism, forestry, trading, and agriculture [50]. The basin is dominated by dense grasslands, shrubs, and scattered tree-type vegetation [53].

2.2. Regional Geology and Hydrogeology

The Komadugu-Yobe basin is a rift basin resulting from basement tensional forces, with a zigzag fault pattern and the absence of other comprehensive physical features [54]. Several factors influence the occurrence of faults including the presence of pre-existing lines of weakness formed during the Pan-African orogenic event [55]. The basin is underlain

by basement-complex rocks and sedimentary quaternary formations (Figure 1). The main geological structures in the basin are faults and simple symmetrical folds that are predominant in a northeast–southwest trend. The faults are dominant in the basement section and result in grabens, horsts, and other related features. Some high-angle faults are formed within the underlying sediment in the sub-basin because of the movement along these basement faults [54]. However, the folds in the Komadugu-Yobe basin comprise simple and folded sediments with low fold frequency and amplitude that flatten with depth. The frequency of folds decreases towards the northwestern part of the basin, while the fold amplitude increases in a southeast direction. The stratigraphic sequence of the sediments in the Komadugu-Yobe basin was presented by Avbovbo et al. [54], Obaje et al. [56], Obaje [57], Lopez et al. [58], and Bura et al. [59].

The quaternary Chad formation is the most recent formation in the basin, a Pliocene-Pleistocene deposit with thick clays of fluviatile and lacustrine origin. It consists of light gray claystone, minor sand, and some infrequent pebbly horizons that exhibit ferruginization in the deposits [18,55,59]. The Keri-Keri formation is characterized by conglomerate, siltstone, grit, sandstone, and clay that overlie the Maastrichtian Fika Shale and Gombe Sandstone. This deposit contains minerals such as zircon, tremolite, pyroxene, rutile, staurolite, kyanite, tourmaline, limonite, and hornblende [59–61]. The Bima sandstone is situated above the Gongila formation. It is derived from the weathering of basement rocks and consists of a sequence of red sandstone and mudstone [59,62]. The Gongila formation is characterized by the presence of substantial layers of calcareous gray to dark shales and silty sandstone, which were deposited in a marine setting. Furthermore, the Fika formation consists of dark-gray to blue-black shale. It has been dated as Turonian-Maastrichtian in age by Obaje [57]. The upper part of the formation infrequently has glauconite, gypsum, and fine-grained sandstone [59].

The Plio-Pleistocene Chad formation and the younger underlying Quaternary sediments are the primary groundwater-bearing units in the basin. Groundwater supply in the basin is provided by the upper, middle, and lower aquifers of the Chad formation, which are separated by thick clay layers. The lower and intermediate aquifers are mostly confined, whereas the upper aquifer is mostly unconfined or partially confined in a few locations [58,59,63–65]. According to Akujieze et al. [66], a yield of 2.5 to 30 L/s is common in the upper aquifer. The yield of the middle and lower aquifers ranges from 24 to 32 L/s and 10 to 35 L/s, respectively [65,66]. The Komadugu-Yobe Valley serves as the main source of recharge for the unconfined Lake Chad quaternary aquifer, mostly through percolation and wetlands. The processes of aquifer recharge and pollution hazard potential have been impacted due to extensive irrigation farming practices within the basin [67,68]. The alluvial aquifer located beneath the Yobe floodplain undergoes recharge through various mechanisms, including seepage from the river channel, infiltration of floodwater, and surplus rainfall. These sources act alone or in combination to replenish the aquifer [11,68]. Carter and Alkali [69] estimated a recharge of 30–60 mm/year around the Manga grasslands of northeastern Nigeria. Moreover, recharge of 14–49 mm/year was estimated by Edmunds et al. [64] in the Komadugu-Yobe basin.

2.3. Groundwater Sampling and Field Measurement

A total of 120 groundwater samples were collected from shallow hand-dug wells and boreholes within the Komadugu-Yobe Basin from August to October 2021. The groundwater sampling location is shown in Figure 1. The groundwater sampling was preformed following the standard procedure [70]. Groundwater was pumped out of the source for 5 min to flush standing water in the borehole before sampling. Sampling was conducted using 50 mL polyethylene bottles. Samples for cations were filtered using a 0.45µm acetate cellulose syringe filter and acidified with 0.4 mL of concentrated nitric acid (HNO_3). Remaining samples were filtered using a 0.45 µm acetate cellulose syringe filter. Samples were sealed to avoid air exposure and stored in ice-packed coolers to maintain a temperature of ~4 °C. The samples were shipped to the Department of Civil and Environmental

Engineering Laboratory, University of Strathclyde, Glasgow for further analysis. The pH, electrical conductivity, and total dissolved solids were measured in situ with a potable digital electrical conductivity meter (Model 99720 pH/Conductivity meter). The water depth was measured with a dip meter, while the geographic coordinates of each sampling location were recorded using a handheld Global Positioning System (GPS).

2.4. Laboratory Analysis

Groundwater samples were analyzed following the standard procedure given by the American Public Health Association [70]. A total of 15 mL of groundwater sample was collected in a 15 mL centrifuge tube from 120 samples (acidified) each and analyzed using inductively coupled plasma optical emission spectrometry (ICP-OES, iCAP 6200; Thermo Fisher Scientific) for analysis of the major cations (Na^+, Ca^{2+}, Mg^{2+}, K^+). Ion chromatography (Metrohm 850 Professional IC) was used to analyze the concentration of the major anions (Cl^-, F^-, $SO_4{}^{2-}$, $NO_3{}^-$) in the groundwater samples. The total alkalinity was analyzed in situ using titration with the HACH digital titrator (Model 16900; HACH International, Loveland, CO, USA).

2.5. Accuracy of Chemical Analysis

The ionic balance error (*IBE*) shown in Equation (1) was employed to check the accuracy of the chemical analysis:

$$IBE\% = \frac{\sum c - \sum a}{\sum c + \sum a} \times 100 \quad (1)$$

where *IBE* denotes the ionic balance error; *c* and *a* denotes the sum of cations and anions concentrations in milliequivalents per liter (meq/L). The standard threshold limit for the *IBE%* is ±10. The *IBE* of the analyzed groundwater samples was between −8.45 and 8.64%.

2.6. Geospatial Analysis

ArcGIS 10.8 was used to develop the spatial distribution maps of various groundwater quality parameters and the groundwater quality index. The IDW interpolation approach was used to develop the spatial distribution maps in the spatial analyst toolbox of ArcGIS. This method was used because it follows a deterministic model approach and fits well with real-world parameters [2,33,71].

2.7. Groundwater Quality Index

The groundwater quality index (GWQI) is a quantitative measure used to determine the suitability of groundwater for human consumption. It involves the aggregation of various water quality characteristics into a single index using mathematical summation [2,25,35]. It is used to elucidate trends in water quality over time. The approach has gained acceptance worldwide and has been employed in assessing the suitability of groundwater for drinking purposes in various regions [2,25,34,35].

Groundwater quality index computation involves four main steps: weight assignment for each groundwater quality parameter, relative weight computation, water quality rating scale computation for each parameter, and computation of the sub-index and groundwater quality index as follows:

- Assigning a weight for each groundwater quality parameter: Weights (*wi*) were assigned to various water quality parameters based on their relative importance to human consumption [34]. Nitrates and fluorides were given the highest weight of 5 due to the vital role they played in groundwater quality evaluation and their significant human health impacts [33,35]. Sodium and potassium were given the least weight because they are less significant in groundwater quality assessment. Table 1 shows the weights assigned to each groundwater quality parameter.

- Computation of relative weight: Equation (2) below was used to calculate the relative weight (*Wi*):

$$Wi = \frac{wi}{\sum_{i}^{n} wi} \quad (2)$$

where *Wi* is the relative weight; *wi* denotes the weights assigned for each parameter; *n* denotes the total number of quality parameters; and *i* is the *i*th parameter.

- Water quality rating scale: The rating scale (*qi*) for each parameter was computed by dividing the determined concentration of each parameter (*ci*) and its respective water quality standard (*Si*) recommended by World Health Organization [72], all multiplied by 100. The *qi* for all the parameters was computed using Equation (3) below:

$$qi = \frac{ci}{Si} \times 100 \quad (3)$$

where *qi* denotes the quality rating; *ci* denotes the concentration of each groundwater quality parameter in mg/L; and *Si* is the WHO guideline value for each parameter.

- Sub-index and groundwater quality index computation: The sub-index (*SIi*) for each parameter and overall groundwater quality index (*GWQI*) were calculated using Equations (4) and (5):

$$SIi = Wi \times qi \quad (4)$$

$$GWQI = \sum_{i=0}^{n} SIi \quad (5)$$

where *SIi* denotes the sub-index of the *i*th water quality parameter; *qi* denotes the quality rating of the *i*th parameter; *n* is the total number of water quality parameters; and *GWQI* is the overall groundwater quality index. The groundwater was classified based on portability in Table 2.

Table 1. Groundwater quality parameters weighing for groundwater quality index computation.

Parameters	Units	WHO [72]	Weight (*wi*)	Relative Weight (*Wi*)
pH	/	6.5–8.5	4	0.095
TDS	mg/L	1000	5	0.119
TH	mg/L $CaCO_3$	500	3	0.071
Na+	mg/L	200	2	0.048
K^+	mg/L	12	2	0.048
Ca^{2+}	mg/L	75	3	0.071
Mg^{2+}	mg/L	50	3	0.071
Cl^-	mg/L	300	4	0.095
HCO_3-	mg/L	250	3	0.071
$SO_4{}^{2-}$	mg/L	250	3	0.071
$NO_3{}^-$	mg/L	50	5	0.119
F^-	mg/L	5	5	0.119
			$\sum wi = 42$	$\sum Wi = 1$

Table 2. Groundwater quality index.

Range of GWQI	Class of Water	Number of Samples	% of Samples
<50	Excellent Water	76	63
50–100	Good Water	32	27
100–200	Poor Water	12	10
200–300	Very Poor Water	/	/
>300	Unsuitable	/	/
	Total	120	100

2.8. Hydrochemical Analysis

The water types, hydrochemical facies, and geochemical mechanisms controlling the chemistry of groundwater in the Komadugu-Yobe basin were identified using the

Piper trilinear diagram, Chadha plot, and the Gibbs diagrams. The Piper diagram was developed using the Geochemist Work Bench (GWB) software 17.0. The Gibbs diagram and the Chadha plot were developed using Origin Pro 2022. These diagrams have been widely used by several researchers [33,34] to understand the various principal mechanisms controlling groundwater chemistry. The Gibbs diagrams are based on two ratios and are calculated using Equations (6) and (7):

$$\text{Gibbs ratio}^{-}\text{I} = \frac{Cl^-}{\left(Cl^- + HCO_3^-\right)} \quad (6)$$

$$\text{Gibbs}^{-}\text{II} = \frac{Na^+ + K^+}{\left(Na^+ + K^+ + Ca^{2+}\right)} \quad (7)$$

Ionic concentrations in meq/L.

3. Results and Discussion

Groundwater quality determines its usability. Various groundwater quality parameters analyzed with their descriptive statistics are presented in Table 3. The results of the analyzed groundwater quality parameters were compared with the WHO [72] guidelines (Tables 1 and 3) to determine the suitability of the groundwater for drinking purpose. The geology of the study region was overlaid on the geospatial distribution maps of groundwater quality parameters to relate the interaction between geology and groundwater quality parameters (Figures 2–4).

Table 3. Statistical summary of the physicochemical parameters of groundwater samples of KYB compared with WHO [72] guidelines.

Parameters	Units	Maximum	Minimum	Mean	WHO [72]		PAMPL
					HDL	MPL	
pH	/	8.24	5.52	7.2	6.5–8.5	8.5	/
EC	µS/cm	2746	15	462	1000	/	5
TDS	mg/L	1757	10	296	1000	1500	2.5
TH	mg/L $CaCO_3$	704	0.8	138	100	500	2
Na^+	mg/L	285	2	36	200	250	2.5
K^+	mg/L	96	0.1	10	12	/	6
Ca^{2+}	mg/L	220	0.2	39	75	200	2
Mg^{2+}	mg/L	58	0.1	9.9	50	150	2.5
$HCO^-{}_3$	mg/L	379	1.5	120	250	500	10.8
Cl^-	mg/L	372	0.7	48	300	600	2.5
$SO_4{}^{2-}$	mg/L	133	0.1	15	250	500	/
$NO_3{}^-$	mg/L	314	ND	42	50	50	30
F^-	mg/L	2.3	ND	0.3	1.5	1.5	2

Note: HDL: highest desirable limit; MPL: maximum permissible limit; PAMPL: percentage above maximum permissible limit.

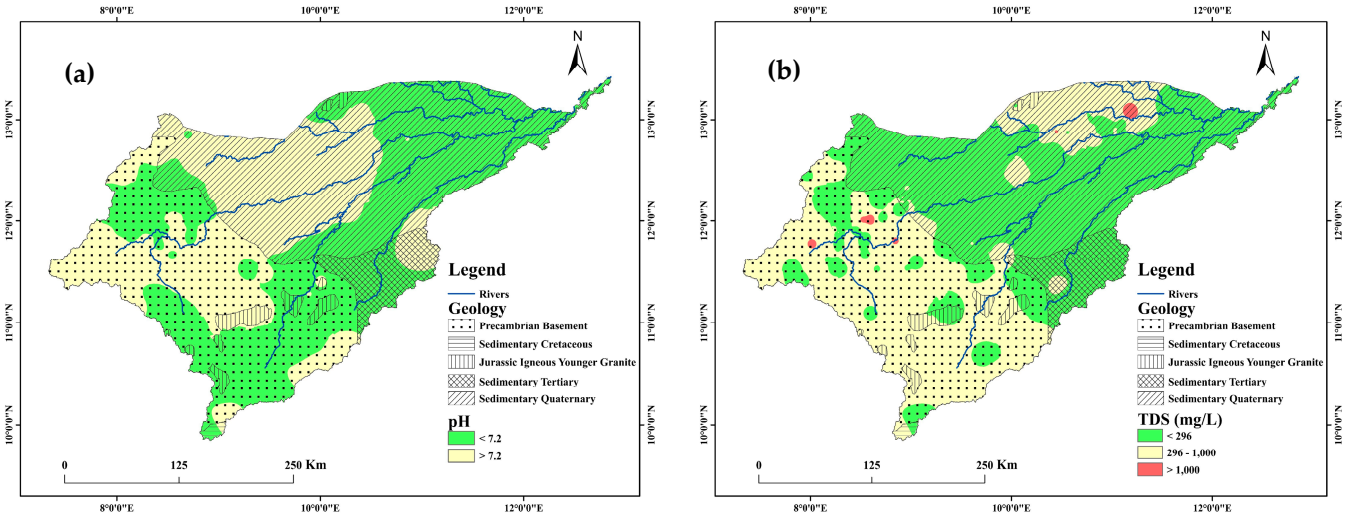

Figure 2. Spatial distribution of groundwater quality parameter in Komadugu-Yobe basin. (**a**) pH; (**b**) TDS.

3.1. Hydrogen Ion Concentration (pH)

pH is an important groundwater quality parameter [34,73]. The pH of the groundwater ranged from 5.52 to 8.24 (Figure 3a), with an average value of 7.2 (Table 2). About 88% of the analyzed samples fall between 6.5 and 8.5, the recommended safe limits prescribed by WHO [72]. Only 12.5% of the analyzed groundwater samples fell below 6.5 indicating some acidic water. A change in pH leads to change in biochemical reactions [71]. Figure 2a shows the eastern part of the basin that is dominated by a sedimentary quaternary formation and exhibits the lowest pH values; meanwhile, the western section, dominated by Precambrian basement, has pH values above the mean value. This could be due to the presence of calcite minerals and alkaline ions from feldspar weathering, which raises the pH of groundwater [74]. However, the low pH values in the sedimentary quaternary may be related to the extensive use of synthetic fertilizers (urea, GDAP, NPK, etc.) during irrigation, which introduced specific compounds that undergo oxidation reactions, resulting in low pH values in groundwater systems.

3.2. Total Dissolved Solids (TDS)

The groundwater in the Komadugu-Yobe basin show variation in concentrations of total dissolved solids (TDSs) (Figure 2b). The TDSs of the groundwater samples vary from 10 to 1757 mg/L, with a mean value of 296 mg/L (Table 2). TDSs are the sum of all dissolved inorganic salts of major ions in water [34]. The method prescribed by Davis and DeWiest [75] was used to classify the groundwater of the study area based on TDS values (Table 4). About 85% of the groundwater sample is desirable for drinking, while 10 and 5% of the groundwater samples are permissible for drinking and useful for irrigation, respectively (Table 4). High TDS values above the mean concentration were observed in the Precambrian basement part of the study area. This is an indicator of the dissolution and weathering of carbonates, salts, and sulfate minerals. Other factors that contribute to high levels of TDS in this region include ion-exchange interaction between ions in the groundwater and ions on the mineral surfaces, as well as groundwater flow through rocks, sediments in the subsurface, and water–rock interaction time. TDS values in the sedimentary quaternary, on the other hand, were lower than the mean concentration. However, high TDSs were observed at the downstream fringes of the basin. This could be attributed to high rates of evaporation than rainfall in the region as well as the anthropogenic impacts from agricultural activities and waste disposal.

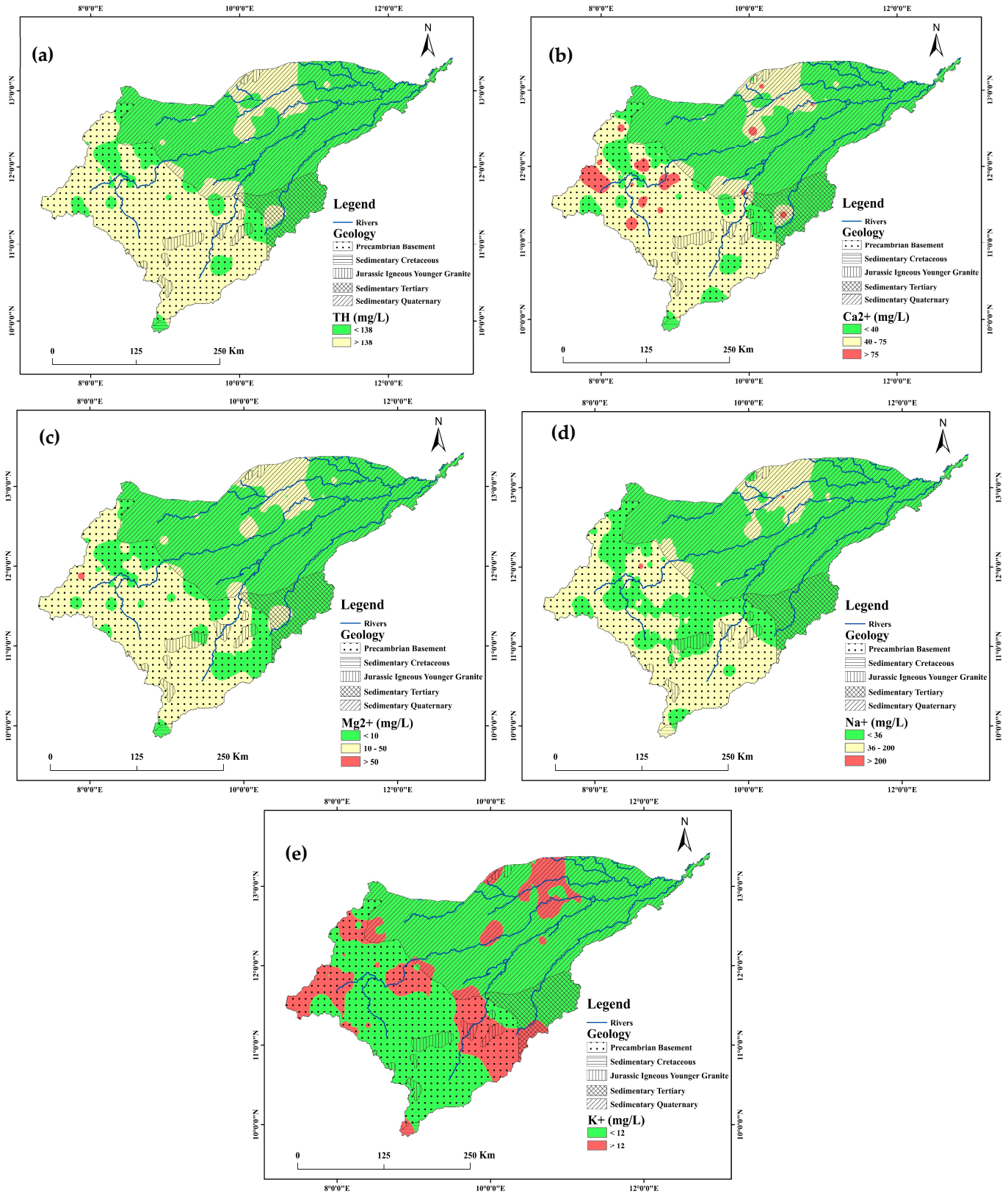

Figure 3. Spatial distribution of groundwater quality parameter in Komadugu−Yobe basin. (**a**) TH; (**b**) Ca^{2+}; (**c**) Mg^{2+}; (**d**) Na^{+}; (**e**) K^{+}.

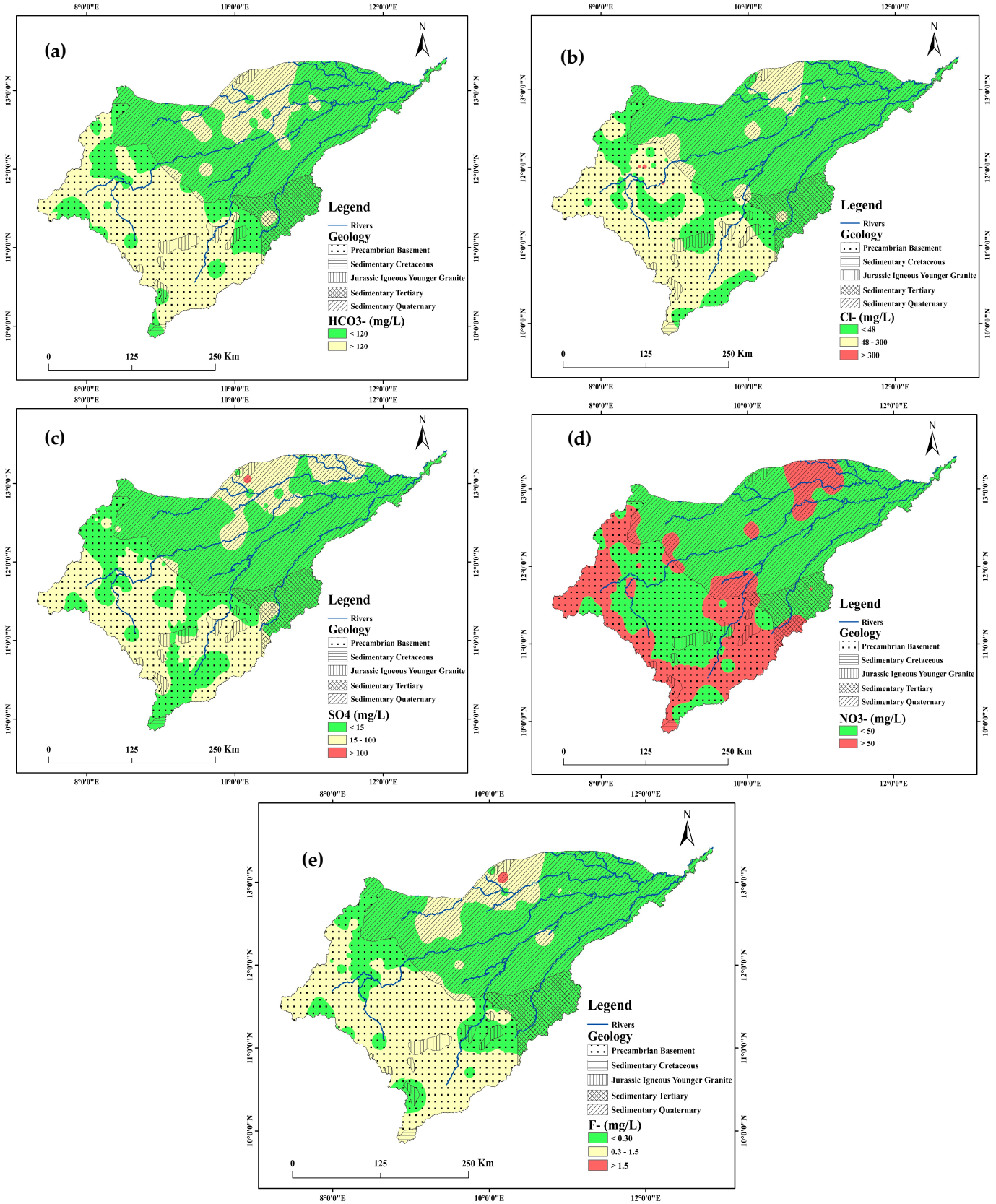

Figure 4. Spatial distribution of groundwater quality parameters in Komadugu−Yobe basin. (**a**) HCO_3^-; (**b**) Cl^-; (**c**) SO_4^{2-}; (**d**) NO_3^-; (**e**) F^-.

Table 4. Groundwater classification based on TDSs [75].

TDS (mg/L)	Class of Groundwater	% of Samples
<500	Desirable for drinking	85
500–1000	Permissible for drinking	10
1000–3000	Useful for irrigation	5
>3000	Unfit for drinking and irrigation	/

3.3. Total Hardness of Water (TH)

Ingestion of water with a high concentration (>300 mg/L) of total hardness (TH) may cause renal failure and the likelihood of the formation of kidney stones due to the presence of calcium carbonate, calcium phosphate, and calcium oxalate [34,51]. The TH of groundwater in the Komadugu-Yobe basin varies from 0.8 to 704 mg/L as $CaCO_3$, with a mean value of 138 mg/L as $CaCO_3$ (Table 2). About 98% of the groundwater samples in the study area were below the maximum permissible limit of 500 mg/L (Table 2). Sawyer and Sawyer & McCarthy [76] classified groundwater based on the concentration of total hardness TH as mg/L of $CaCO_3$ (Table 5). The table shows that about 43% of the groundwater samples in the study area are soft water, whereas 13% of the groundwater samples are in the very hard water category. The spatial distribution of TH in the study area is presented in Figure 3a. The figure reveals that TH concentrations above the mean value were concentrated in the Precambrian basement part, while the sedimentary quaternary section of the basin is dominated by TH concentrations below the mean value. This may be attributed to the presence of calcite and dolomite minerals in the Precambrian basement part of the study area.

Table 5. Total hardness classification based on Sawyer and McCarthy [76].

Water Class	TH as $CaCO_3$ (mg/L)	% of Samples
Soft water	<75	43
Moderately hard water	75–150	18
Hard water	150–300	26
Very hard water	> 300	13

3.4. Calcium (Ca^{2+}) and Magnesium (Mg^{2+})

Calcium (Ca^{2+}) and magnesium (Mg^{2+}) concentrations in groundwater samples of the study area range from 0.2 to 220 mg/L with a mean value of 39 mg/L and from 0.1 mg/L to 58 mg/L with a mean value of 9.9 mg/L, respectively (Table 2). About 2.5% of the groundwater samples were above the World Health Organization [72] maximum permissible limit of Mg^{2+} of 150 mg/L (Table 2). Calcium is derived from cation exchange processes and carbonate dissolution [34]. Therefore, Ca^{2+} variations in groundwater samples could be due to carbonate rock dissolution and ion exchange processes in the Precambrian basement parts of the basin (Figure 3b). Figure 3c depicts the spatial variation in Mg^{2+} in the study area. Furthermore, the lower value of Mg^{2+} concentration in the sedimentary quaternary portion of the basin may be because of the absence of magnesium-bearing minerals in the groundwater of the region. The result also reveals a higher concentration of Ca^{2+} than Mg^{2+}, which could be due to the influence of ion exchange mechanisms and dissolution of mafic minerals in the groundwater system [77]. This is evident in the Precambrian basement parts of the study area.

3.5. Sodium (Na^{+}) and Potassium (K^{+})

Sodium concentration in the groundwater of the study area varies from 2 to 285 mg/L, with a mean value of 36 mg/L (Table 2). About 2.5% of the groundwater samples are above the maximum permissible limit, while 74% of the groundwater samples have concentrations below the mean concentration (Table 2). A high Na^{+} concentration above 200 mg/L

give an unacceptable taste and make water unsuitable for domestic purposes [2,33,70]. The spatial distribution map of Na^+ in the study area is presented in Figure 4d. The concentration of K^+ in the groundwater of the study area varies from 0.1 to 96 mg/L with a mean value of 10 mg/L (Table 2). Approximately 6% of groundwater samples have K^+ concentrations above the WHO [72] maximum permissible limit (Table 2). Potassium is the most important element for human nutrition, with 10 mg/L in natural water [34,70]. Figure 3e shows the spatial distribution of K^+ in KYB, with the sedimentary quaternary Chad formation region characterized by low K^+ concentrations and higher concentrations are dominated in the Precambrian basement portion. This could be attributed to the presence of minerals in the Precambrian basement such as feldspar which releases K^+ ions into the groundwater during weathering. Relatively low concentrations of sodium were observed in the sedimentary Chad formation parts of the basin, whereas the western part, where the geology is Precambrian basement, has a higher concentration of Na^+ (Figure 3d), and low Ca^{2+} (Figure 3b). The cation exchange process of Na^+ with cations on the surface of minerals that replaces Ca^{2+} with Na^+ and the rock–water interaction in the groundwater system of the basin may be due to the high Na^+ concentration. Moreover, high concentrations of Na^+ and K^+ were observed in the downstream rim of the basin due to intensive agricultural activities and the evaporative nature of the sedimentary quaternary portion of the study area.

3.6. Bicarbonate (HCO^-_3)

The concentration of bicarbonate (HCO^-_3) in the groundwater samples of the KYB varies from 1.5 mg/L to 379 mg/L, with a mean value of 120 mg/L (Table 2). Bicarbonate in groundwater is known to have no adverse health effects [33,34]. The WHO [72] guideline for HCO^-_3 concentration in drinking water is 250 mg/L. Only 10.8% of the groundwater have a bicarbonate concentration exceeding the threshold limit of 250 mg/L (Table 2). The spatial distribution of bicarbonate concentration shows an elevated level of HCO^-_3 in the Precambrian basement part, while lower concentrations were observed in the sedimentary quaternary Chad formation region of the study area (Figure 4a). The dissolution and weathering of calcite and dolomite minerals increases the concentration of bicarbonate ions in the groundwater in the Precambrian basement. A few spots in the sedimentary quaternary section of the study area show elevated levels of bicarbonate concentrations due to agricultural activities, which enhance the natural contents of bicarbonate ions in the groundwater system [78].

3.7. Chloride (Cl^-) and sulfate ($SO_4{}^{2-}$)

The concentration of chloride (Cl^-) and sulfate ($SO_4{}^{2-}$) in the groundwater of the KYB varies from 0.7 to 372 mg/L, with a mean concentration of 48 mg/L, and from 0.1 to 133 mg/L, with a mean value of 15 mg/L, respectively (Table 2). Excessive chlorine in drinking water imparts a salty taste and signifies contamination from various natural and anthropogenic sources [34]. Chloride concentrations in about 2.5% of the groundwater samples exceeded the WHO guidelines for drinking water (Table 2). However, most of the groundwater samples have a Cl^- concentration above 50 mg/L. These high chloride concentrations may be attributed to pollution from domestic and industrial waste, leachate from dumpsites and septic tanks, animal waste, and agricultural fertilizer [33,70]. The spatial distribution of chloride concentration in the groundwater of the study area is presented in Figure 4b. Low Cl^- concentration was observed in the sedimentary quaternary Chad formation part of the study area except in a few locations receiving chlorides from agricultural practices and domestic waste, while the Precambrian basement portion is dominated by high Cl^- concentrations due to infiltration of chloride-bearing pollutant into the groundwater system. The spatial distribution of sulfate concentration in the groundwater of the study area is shown in Figure 4c. The WHO [72] guideline value for sulfate $SO_4{}^{2-}$ in drinking water is 250 mg/L. All the groundwater samples are below the maximum permissible limit (Table 2, WHO, [72]). Sulfates in the groundwater of the

sedimentary quaternary parts of the basin are from the natural process of evaporation and anthropogenic activities such as artificial fertilizer applications, industrial effluents, and municipal waste. Meanwhile, the sulfate concentration in the Precambrian basement region could be from the dissolution of gypsum and other sulfate-bearing minerals in the groundwater systems [79].

3.8. Nitrate (NO_3^-) and Fluoride (F^-)

Groundwater NO_3^- contamination is an important water quality issue globally [33–35,72]. Nitrate in the groundwater arises from synthetic fertilizers and organic manures, leachate from dumpsites, septic tanks, landfills, and industrial and municipal waste [73]. The nitrate concentration in Komadugu-Yobe basin varies from ND to 314 mg/L, with a mean value of 42 mg/L (Table 2). The maximum permissible limit of NO_3^- concentration in drinking water is 50 mg/L [72]. Groundwater with nitrate concentrations higher than the maximum permissible limits have been linked to an increased risk of methemoglobinemia [34,72]. About 30% of the groundwater samples were above the WHO guidelines for nitrate (Table 2). The spatial distribution of nitrate in KYB is presented in Figure 4d. It is worth noting that high nitrate concentrations are visible in the Precambrian basement and the sedimentary quaternary formation of the study area. These high concentrations came from various anthropogenic pollutions in the study area as well as denitrification processes in the sedimentary parts of the study area.

The concentration of F^- in the groundwater samples varies from ND to 2.3 mg/L, with a mean value of 0.3 mg/L (Table 2). About 2% of the groundwater samples have a F^- concentration exceeding the maximum permissible limit (Table 2, WHO, [72]), which renders them unsuitable for drinking purposes. Figure 4e shows the spatial distribution of fluoride in groundwater of KYB. The sedimentary Chad formation has groundwater with predominantly low fluoride concentrations, whereas elevated fluoride concentrations were observed in the Precambrian basement part of the basin. The dissolution of fluoride-bearing minerals and geothermal activities could be the possible source of fluoride in the Precambrian basement parts of the basin. Previous studies in Nigeria such as Akpata et al. [80], Giwa et al. [81], Malago et al. [82], and Waziri et al. [83] have suggested that high fluoride concentrations in northeastern and northwestern Nigeria are due to overexploitation of basement and quaternary aquifers. Ingestion of groundwater with high fluoride concentrations could lead to dental and skeletal fluorosis [84,85]. Therefore, there is a need for further study of the risks associated with groundwater fluoride in the study area.

3.9. Geochemical Mechanism of Groundwater

Gibbs [86] showed that groundwater chemistry is controlled by three main natural processes: rock weathering/rock–water interaction, evaporation, and atmospheric precipitation. A Gibbs plot [86] reveals the interaction between groundwater, soil, and host rock [25,73,87]. Figure 5 presents the Gibbs plot of the Komadugu-Yobe basin, indicating groundwater chemistry is mainly controlled by rock weathering/rock–water interaction. The Gibbs ratios of the cations and anions of the groundwater varies from 0.2 to 0.95 and 0.1 to 0.9, with an average of 0.5 and 0.2, respectively, and suggest the area is dominated by silicate minerals [33,82]. Only 8% of the groundwater samples indicated precipitation and evaporation, and given the semi-arid climates, some evaporation in the northeastern part of KYB where the geology is sedimentary quaternary may also affect the chemistry of the groundwater.

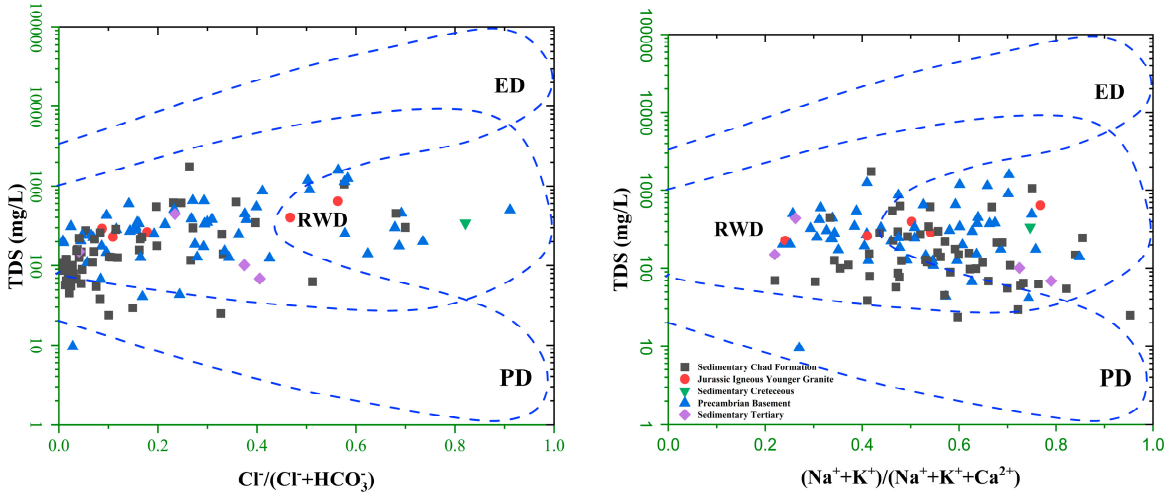

Figure 5. Gibbs plots showing the dominant geochemical mechanisms in KYB, (**left**): anions ratio and (**right**): cations ratio vs. TDS (mg/L). ED: evaporation dominance. RWD: rock weathering dominance. PD: precipitation dominance.

3.10. Groundwater Types and Hydrogeochemical Evolution

3.10.1. Piper Plot

The Piper trilinear diagram (Figure 6) for the Komadugu−Yobe basin uses major ions to classify groundwater into various hydrochemical types and identify influential factors involved in groundwater chemistry [23,24,88]. Figure 6 shows the cations of the groundwater are plotted in the calcium and sodium zones, while the anions are mainly plotted in the bicarbonate and chloride zone. About 59% of the groundwater samples were plotted in the Ca^{2+}-Mg^{2+}-HCO^{-}_{3} water type. The order of dominance of the groundwater type in the basin is Ca^{2+}-Mg^{2+}-HCO^{-}_{3} > Na^{+}-Cl^{-} > Na^{+}-HCO^{-}_{3} > Ca^{2+}-Mg^{2+}-$SO_4{}^{2-}$-Cl^{-}. These show that the hydrochemical types resulted from the dissolution of carbonate-rich minerals and the weathering of silicate minerals within the aquifer systems of the Precambrian basement parts of the basin. The presence of a few Na^{+}-Cl^{-} and Na^{+}-HCO^{-}_{3} water types may be due to rainfed agricultural activities taking place in both Precambrian and sedimentary quaternary parts of the study area. It is strongly believed that Na^{+}-HCO^{-}_{3} enhances the presence and dissolution of fluoride in groundwater systems, particularly in the Precambrian basement geologic formation [23,33,70].

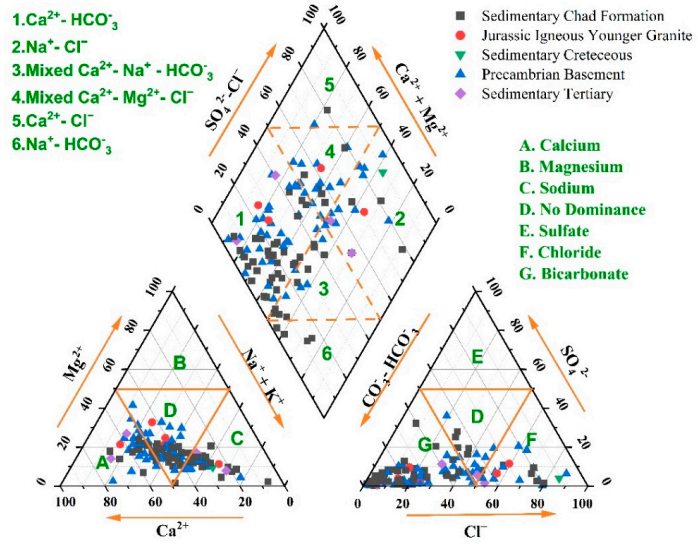

Figure 6. Piper diagram showing various water types in Komadugu−Yobe basin.

3.10.2. Chadha Diagram

The Chadha diagram was employed to assessed the geochemistry of groundwater and various groundwater types in the Komadugu-Yobe basin. The Chadha plot shows the presence of Ca^{2+}-Mg^{2+}-HCO^{-}_3, Ca^{2+}-Mg^{2+}-$SO_4{}^{2-}$-Cl^{-}, Na^{+}-Cl^{-}, and Na^{+}-HCO^{-}_3 water types in the study area (Figure 7). The Chadha diagram is a composite representation that integrates the Piper plot and the extended Durov diagram [23]. The Chaha plot best describes the permanent and temporary hardness domains of water [73]. Figure 7 reveals that the alkaline earths exceeded the alkali metals and weak acids exceeded strong acids in the groundwater samples of KYB. The Chadha plot shows over half of the groundwater facies belong to the Ca^{2+}–Mg^{2+}– HCO^{-}_3 water type with temporary hardness dominated in the Precambrian basement parts of the study area. However, Na^{+}– HCO^{-}_3, Na^{+}– Cl^{-}, and Ca^{2+}– Mg^{2+}– Cl^{-} water types were also present in the groundwater of KYB. This could be attributed to dissolution and weathering of calcite and dolomite minerals in the Precambrian basement parts, as well as the influence of evaporation and anthropogenic activities in the sedimentary quaternary Chad formation section of the study area. This result agrees with what was observed in the Piper trilinear diagram (Figure 6).

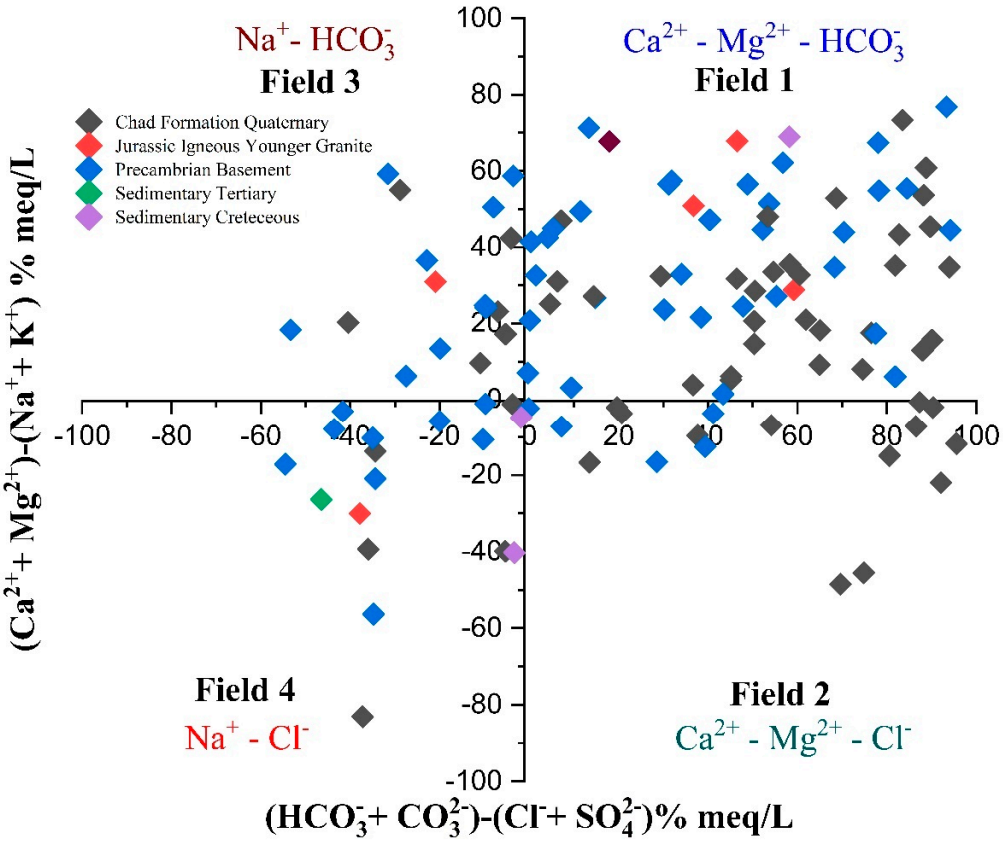

Figure 7. Chada plot showing groundwater evolution in Komadugu−Yobe basin.

3.11. Groundwater Quality Index

The spatial distribution of the groundwater quality index in the Komadugu−Yobe basin is presented in Figure 8 and varies from 9 to 170, with an average value of 48 (Table 6). Groundwater in the study area can be categorized into five classes based on GWQI values: excellent water (GWQI < 50), good water (GWQI = 50–100), poor water (GWQI = 100–200), very poor water (GWQI = 200–300), and unfit for drinking (GWQI > 300) [33,34]. The majority of the groundwater in KYB is excellent, constituting about 63%, with good and poor water classes constituting 27% and 10% respectively (Table 2, Figure 9). It was observed that the poor groundwater quality occurs in the Precambrian basement portion of the basin. This could be attributed to geogenic processes including weathering and

dissolution of minerals, as well as anthropogenic pollution resulting from the extensive use of artificial fertilizers, indiscriminate discharge of effluent from local industries, leachates from dumpsites, septic tanks, and pit latrines.

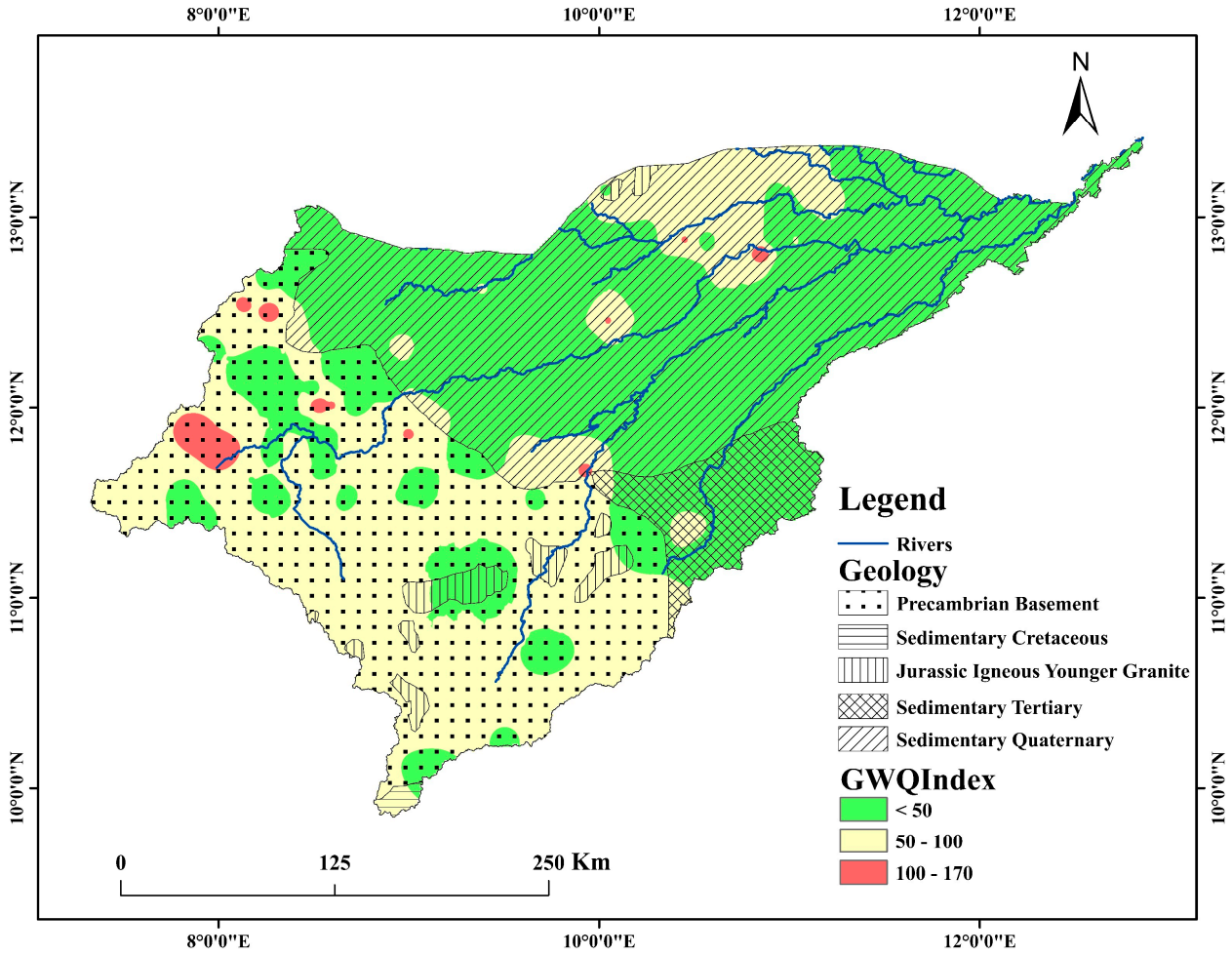

Figure 8. Spatial distribution of groundwater quality index in Komadugu−Yobe basin.

Table 6. Groundwater quality index (GWQI) in Komadugu−Yobe basin.

Sample Numbers	GWQI	Water Type	Sample Numbers	GWQI	Water Type
L1	79	Good Water	L63	74	Good Water
L2	49	Excellent Water	L64	51	Good Water
L3	74	Good Water	L65	125	Poor Water
L4	104	Poor Water	L66	76	Good Water
L5	41	Excellent Water	L67	9	Excellent Water
L6	82	Good Water	L68	62	Good Water
L7	20	Excellent Water	L69	15	Excellent Water
L8	18	Excellent Water	L70	20	Excellent Water
L9	24	Excellent Water	L71	62	Good Water
L10	82	Good Water	L72	46	Excellent Water
L11	39	Excellent Water	L73	38	Excellent Water
L12	29	Excellent Water	L74	61	Good Water
L13	18	Excellent Water	L75	41	Excellent Water
L14	17	Excellent Water	L76	49	Excellent Water

Table 6. *Cont.*

Sample Numbers	GWQI	Water Type	Sample Numbers	GWQI	Water Type
L15	19	Excellent Water	L77	61	Good Water
L16	14	Excellent Water	L78	73	Good Water
L17	156	Poor Water	L79	37	Excellent Water
L18	20	Excellent Water	L80	67	Good Water
L19	31	Excellent Water	L81	91	Good Water
L20	25	Excellent Water	L82	38	Excellent Water
L21	19	Excellent Water	L83	14	Excellent Water
L22	15	Excellent Water	L84	79	Good Water
L23	31	Excellent Water	L85	52	Good Water
L24	59	Good Water	L86	64	Good Water
L25	91	Good Water	L87	38	Excellent Water
L26	134	Poor Water	L88	15	Excellent Water
L27	170	Poor Water	L89	18	Excellent Water
L28	49	Excellent Water	L90	15	Excellent Water
L29	36	Excellent Water	L91	16	Excellent Water
L30	28	Excellent Water	L92	13	Excellent Water
L31	107	Poor Water	L93	17	Excellent Water
L32	150	Poor Water	L94	107	Poor Water
L33	14	Excellent Water	L95	58	Good Water
L34	37	Excellent Water	L96	30	Excellent Water
L35	27	Excellent Water	L97	14	Excellent Water
L36	65	Good Water	L98	14	Excellent Water
L37	107	Poor Water	L99	32	Excellent Water
L38	101	Poor Water	L100	26	Excellent Water
L39	23	Excellent Water	L101	103	Poor Water
L40	22	Excellent Water	L102	24	Excellent Water
L41	38	Excellent Water	L103	23	Excellent Water
TL42	83	Good Water	L104	50	Good Water
L43	34	Excellent Water	L105	18	Excellent Water
L44	64	Good Water	L106	40	Excellent Water
L45	49	Excellent Water	L107	30	Excellent Water
L46	32	Excellent Water	L108	33	Excellent Water
L47	58	Good Water	L109	28	Excellent Water
L48	71	Good Water	L110	52	Good Water
L49	23	Excellent Water	L111	25	Excellent Water
L50	32	Excellent Water	L112	19	Excellent Water
L51	39	Excellent Water	L113	18	Excellent Water
L52	27	Excellent Water	L114	24	Excellent Water
L53	40	Excellent Water	L115	58	Good Water
L54	54	Good Water	L116	16	Excellent Water
L55	110	Poor Water	L117	12	Excellent Water
L56	35	Excellent Water	L118	11	Excellent Water
L57	33	Excellent Water	L119	35	Excellent Water
L58	72	Good Water	L120	94	Good Water
L59	24	Excellent Water	Maximum	170	/
L60	36	Excellent Water	Minimum	9	/
L61	33	Excellent Water	Mean	48	/
L62	84	Good Water			

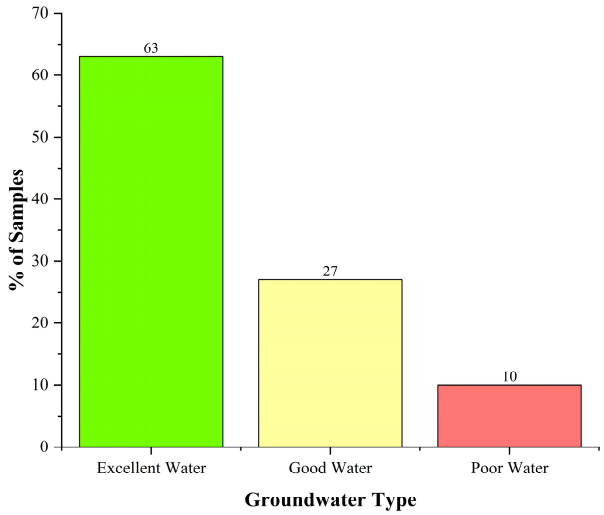

Figure 9. Groundwater quality index (GWQI) classification in Komadugu−Yobe basin.

4. Conclusions

This study presents the hydrogeochemical characteristics and suitability of groundwater resources for drinking purposes in the Komadugu-Yobe basin, Sahel region. This study analyzed 120 groundwater samples to determine the hydrogeochemical characteristics and overall quality of groundwater in KYB using a Gibbs plot, hydrochemical facies plots, and groundwater quality index. The following are the key conclusions from this study:

- The order of the abundance of the major cations and anions in the groundwater samples is: $Ca^{2+} > Na^{+} > K^{+} > Mg^{2+}$ and $HCO^{-}{}_{3} > Cl^{-} > NO_{3}{}^{-} > SO_{4}{}^{2-} > F^{-}$, respectively. More than 90% of groundwater samples have Na^{+}, Ca^{2+}, Mg^{2+}, K^{+}, Cl^{-}, and $SO_{4}{}^{2-}$ and total hardness within the WHO [72] maximum permissible limits. However, some locations show high F^{-} and $NO_{3}{}^{-}$ concentrations, largely in the Precambrian basement region and a few locations in the sedimentary formation parts of the study area.
- The chemistry of the major ions in the groundwater samples of the study area is predominantly (92%) influenced by weathering/rock–water interaction.
- Ca^{2+}-Mg^{2+}-$HCO^{-}{}_{3}$ is the most prevalent hydrochemical facies of groundwater in KYB accounting for more than half (59%) of the groundwater samples. The order of dominance of the groundwater type of the study region is Ca^{2+}-Mg^{2+}-$HCO^{-}{}_{3}$ > Na^{+}-Cl^{-} > Na^{+}-$HCO^{-}{}_{3}$ > Ca^{2+}-Mg^{2+}-$SO_{4}{}^{2-}$-Cl^{-}. The Na^{+}-$HCO^{-}{}_{3}$ groundwater type may promote fluoride dissolution, perhaps contributing to fluoride enrichment in groundwater in some parts of the Precambrian basement complex and the sedimentary Chad formation of the study area. The Piper trilinear plot findings agree with the Chadha diagram results.
- Based on GWQI, the groundwater in the study area is generally of excellent (63%) to good quality (27%) with only 10% exhibiting poor quality. The Precambrian basement complex region of the study basin has the most significant presence of good and poor water quality classes.

Author Contributions: Conceptualization, A.S. and R.M.K.; methodology, A.S.; software, A.S., L.C.B., and I.M.L.; validation, A.S., R.M.K. and V.P.; formal analysis, A.S.; investigation, A.S.; resources, A.S.; data curation, A.S.; writing—original draft preparation, A.S.; writing—review and editing, A.S., R.M.K., V.P., L.C.B. and I.M.L.; visualization, L.C.B. and I.M.L.; supervision, R.M.K. and V.P.; project administration, A.S.; funding acquisition, R.M.K. and A.S. All authors have read and agreed to the published version of the manuscript.

Funding: This research was funded by the Petroleum Technology Development Fund (PTDF) under the Overseas Ph.D. scholarship scheme and supported through funding from the Scottish Government under the Climate Justice Fund Water Futures Program (research grant HN-CJF-03), which was awarded to the University of Strathclyde (Prof. R.M. Kalin).

Data Availability Statement: The data presented in this study are available on request from the corresponding author.

Acknowledgments: The authors are grateful to Auwalu Bello Aliyu, Musa Aliyu Danrumpha, Abdulrahman Sulaiman, Mara Knapp, and Tatyana Peshkur for providing help during fieldwork and laboratory analysis.

Conflicts of Interest: The authors declare no conflicts of interest.

References

1. Ganiyu, S.A.; Mabunmi, A.A.; Olurin, O.T.; Adeyemi, A.A.; Jegede, O.A.; Okeh, A. Assessment of microbial and heavy metal contamination in shallow hand-dug wells bordering Ona River, Southwest Nigeria. *Environ. Monit. Assess.* **2021**, *193*, 126. [CrossRef]
2. Kawo, N.S.; Karuppannan, S. Groundwater quality assessment using water quality index and GIS technique in Modjo River Basin, central Ethiopia. *J. African Earth Sci.* **2018**, *147*, 300–311. [CrossRef]
3. Namara, R.E.; Hanjra, M.A.; Castillo, G.E.; Ravnborg, H.M.; Smith, L.; Van Koppen, B. Agricultural water management and poverty linkages. *Agric. Water Manag.* **2010**, *97*, 520–527. [CrossRef]
4. Solangi, G.S.; Siyal, A.A.; Babar, M.M.; Siyal, P. Groundwater quality evaluation using the water quality index (WQI), the synthetic pollution index (SPI), and geospatial tools: A case study of Sujawal district, Pakistan. *Hum. Ecol. Risk Assess.* **2020**, *26*, 1529–1549. [CrossRef]
5. Li, P.Y.; Qian, H.; Wu, J.H.; Ding, J. Geochemical modeling of groundwater in southern plain area of Pengyang County, Ningxia, China. *Water Sci. Eng.* **2010**, *3*, 282–291. [CrossRef]
6. Mostafa, M.G.; Uddin, S.M.H.; Haque, A.B.M.H. Assessment of hydro-geochemistry and groundwater quality of Rajshahi City in Bangladesh. *Appl. Water Sci.* **2017**, *7*, 4663–4671. [CrossRef]
7. Ganiyu, S.A.; Badmus, B.S.; Olurin, O.T.; Ojekunle, Z.O. Evaluation of seasonal variation of water quality using multivariate statistical analysis and irrigation parameter indices in Ajakanga area, Ibadan, Nigeria. *Appl. Water Sci.* **2018**, *8*, 1–15. [CrossRef]
8. Trabelsi, R.; Zouari, K. Coupled geochemical modeling and multivariate statistical analysis approach for the assessment of groundwater quality in irrigated areas: A study from North Eastern of Tunisia. *Groundw. Sustain. Dev.* **2019**, *8*, 413–427. [CrossRef]
9. Loh, Y.S.A.; Akurugu, B.A.; Manu, E.; Aliou, A.S. Assessment of groundwater quality and the main controls on its hydrochemistry in some Voltaian and basement aquifers, northern Ghana. *Groundw. Sustain. Dev.* **2020**, *10*, 100296. [CrossRef]
10. Rivett, M.O.; Miller, A.V.; MacAllister, D.J.; Fallas, A.; Wanangwa, G.J.; Mleta, P.; Phiri, P.; Mannix, N.; Monjerezi, M.; Kalin, R.M. A conceptual model based framework for pragmatic groundwater-quality monitoring network design in the developing world: Application to the Chikwawa District, Malawi. *Groundw. Sustain. Dev.* **2018**, *6*, 213–226. [CrossRef]
11. Goes, B.J.M. Estimate of shallow groundwater recharge in the Hadejia-Nguru Wetlands, semi-arid northeastern Nigeria. *Hydrogeol. J.* **1999**, *7*, 294–304. [CrossRef]
12. Goni, I.B.; Sheriff, B.M.; Kolo, A.M.; Ibrahim, M.B. Assessment of nitrate concentrations in the shallow groundwater aquifer of Maiduguri and environs, Northeastern Nigeria. *Sci. African* **2019**, *4*, e00089. [CrossRef]
13. Jagaba, A.H.; Kutty, S.R.; Hayder, G.; Baloo, L.; Abubakar, S.; Ghaleb, A.A.; Lawal, I.M.; Noor, A.; Umaru, I.; Almahbashi, N.M. Water quality hazard assessment for hand dug wells in Rafin Zurfi, Bauchi State, Nigeria. *Ain Shams Eng. J.* **2020**, *11*, 983–999. [CrossRef]
14. Wali, S.U.; Alias, N.; Bin, S. Reevaluating the hydrochemistry of groundwater in basement complex aquifers of Kaduna Basin, NW Nigeria using multivariate statistical analysis. *Environ. Earth Sci.* **2021**, *80*, 208. [CrossRef]
15. Balogun, M.A.; Anumah, A.O.; Adegoke, K.A.; Maxakato, N.W. *Environmental Health Impacts and Controlling Measures of Anthropogenic Activities on Groundwater Quality in Southwestern Nigeria*; Springer International Publishing: Berlin/Heidelberg, Germany, 2022; Volume 194. [CrossRef]
16. Ocheri, M.; Odoma, L.; Umar, N. Groundwater Quality in Nigerian Urban Areas: A Review. *Glob. J. Sci. Front. Res.* **2014**, *14*, 35–46. Available online: http://journalofscience.org/index.php/GJSFR/article/view/1293 (accessed on 14 February 2024).
17. Stephen, U.N.; Celestine, O.O.; Solomon, O.O. Analysis of hydrogeochemical facies in groundwater of upper part of Cross River Basin, southeastern Nigeria. *J. African Earth Sci.* **2017**, *131*, 145–155. [CrossRef]
18. Wali, S.U.; Dankani, I.M.; Abubakar, S.D.; Gada, M.A.; Usman, A.A.; Shera, I.M.; Umar, K.J. Review of groundwater potentials and groundwater hydrochemistry of semi-arid Hadejia-Yobe Basin, North-Eastern Nigeria. *J. Geol. Res.* **2020**, *2*, 20–33. [CrossRef]
19. Masood, A.; Aslam, M.; Bao, Q.; Warish, P.; Sarfaraz, K. Integrating water quality index, GIS and multivariate statistical techniques towards a better understanding of drinking water quality Bureau of Indian Standards. *Environ. Sci. Pollut. Res.* **2021**, *29*, 26860–26876. [CrossRef] [PubMed]

20. Omonona, O.V.; Amah, J.O.; Olorunju, S.B.; Waziri, S.H.; Ekwe, A.C.; Umar, D.N.; Olofinlade, S.W. Hydrochemical characteristics and quality assessment of groundwater from fractured Albian carbonaceous shale aquifers around Enyigba-Ameri, southeastern Nigeria. *Environ. Monit. Assess.* **2019**, *191*, 1–22. [CrossRef] [PubMed]
21. Nalami, Z.M.; Ibrahim, M.; Usman, A. The Effect of Hadejia- Jama' are River Basin Development Authority on Dry Season Farming in Kura Local Government Area of Kano State, Nigeria. *Sci. Pap. Manag. Econ. Eng. Agric. Rural. Dev.* **2019**, *19*, 215–220.
22. Ezugwu, C.K.; Onwuka, O.S.; Egbueri, J.C.; Unigwe, C.O.; Ayejoto, D.A. Multi-criteria approach to water quality and health risk assessments in a rural agricultural province, southeast Nigeria. *HydroResearch* **2019**, *2*, 40–48. [CrossRef]
23. Wagh, V.M.; Mukate, S.V.; Panaskar, D.B.; Muley, A.A.; Sahu, U.L. Study of groundwater hydrochemistry and drinking suitability through Water Quality Index (WQI) modelling in Kadava river basin, India. *SN Appl. Sci.* **2019**, *1*, 1–16. [CrossRef]
24. Xiao, Y.; Hao, Q.; Xiao, D.; Zhu, Y.; Yin, S.; Zhang, Y. Hydrogeochemical insights into the signatures, genesis and sustainable perspective of nitrate enriched groundwater in the piedmont of Hutuo watershed, China. *Catena* **2022**, *212*, 106020. [CrossRef]
25. Adimalla, N.; Li, P.; Venkatayogi, S. Hydrogeochemical Evaluation of Groundwater Quality for Drinking and Irrigation Purposes and Integrated Interpretation with Water Quality Index Studies. *Environ. Process.* **2018**, *5*, 363–383. [CrossRef]
26. Kalin, A.; Long, R.M. Application of hydrogeochemical modelling for validation of hydrologie flow modelling in the Tucson basin aquifer, Arizona, United States of America. In Proceedings of the a Final Research Co-ordination Meeting Held, Vienna, Austria, 1–4 June 1993; pp. 147–178.
27. Kalin, R.M. Manual on mathematical models in isotope hydrogeology. In *Chapter 4: Basic Concepts and Formulations for Isotope-geochemical Process Investigations, Procedures and Methodologies of Geochemical Modelling of Groundwater Systems*; IAEA: Vienna, Autria, 1995; pp. 155–206. Available online: http://scholar.google.com/scholar?hl=en&btnG=Search&q=intitle:Manual+on+mathematical+models+in+isotope+hydrogeology#0 (accessed on 14 February 2024).
28. Marini, L. *Geological Sequestration of Carbon Dioxide: Thermodynamics, Kinetics, and Reaction Path Modeling*; Elsevier: Amsterdam, The Netherlands, 2006.
29. Ahmed, N.; Bodrud-Doza, M.; Islam, S.D.; Choudhry, M.A.; Muhib, M.I.; Zahid, A.; Hossain, S.; Moniruzzaman, M.; Deb, N.; Bhuiyan, M.A. Hydrogeochemical evaluation and statistical analysis of groundwater of Sylhet, north-eastern Bangladesh. *Acta Geochim.* **2019**, *38*, 440–455. [CrossRef]
30. Mgbenu, C.N.; Egbueri, J.C. The hydrogeochemical signatures, quality indices and health risk assessment of water resources in Umunya district, southeast Nigeria. *Appl. Water Sci.* **2019**, *9*, 1–19. [CrossRef]
31. Tiwari, A.K.; Singh, A.K.; Singh, A.K.; Singh, M.P. Hydrogeochemical analysis and evaluation of surface water quality of Pratapgarh district, Uttar Pradesh, India. *Appl. Water Sci.* **2017**, *7*, 1609–1623. [CrossRef]
32. Egbueri, J.C. Heavy Metals Pollution Source Identification and Probabilistic Health Risk Assessment of Shallow Groundwater in Onitsha, Nigeria. *Anal. Lett.* **2020**, *53*, 1620–1638. [CrossRef]
33. Vaiphei, S.P.; Kurakalva, R.M.; Sahadevan, D.K. Water quality index and GIS-based technique for assessment of groundwater quality in Wanaparthy watershed, Telangana, India. *Environ. Sci. Pollut. Res.* **2020**, *27*, 45041–45062. [CrossRef] [PubMed]
34. Adimalla, N.; Taloor, A.K. Hydrogeochemical investigation of groundwater quality in the hard rock terrain of South India using Geographic Information System (GIS) and groundwater quality index (GWQI) techniques. *Groundw. Sustain. Dev.* **2020**, *10*, 100288. [CrossRef]
35. Aladejana, J.A.; Kalin, R.M.; Sentenac, P.; Hassan, I. Groundwater quality index as a hydrochemical tool for monitoring saltwater intrusion into coastal freshwater aquifer of Eastern Dahomey Basin, Southwestern Nigeria. *Groundw. Sustain. Dev.* **2021**, *13*, 100568. [CrossRef]
36. Olasoji, S.O.; Oyewole, N.O.; Abiola, B.; Edokpayi, J.N. Water quality assessment of surface and groundwater sources using a water quality index method: A case study of a peri-urban town in southwest, Nigeria. *Environments* **2019**, *6*, 23. [CrossRef]
37. Qasemi, M.; Darvishian, M.; Nadimi, H.; Gholamzadeh, M.; Afsharnia, M.; Farhang, M.; Allahdadi, M.; Darvishian, M.; Zarei, A. Characteristics, water quality index and human health risk from nitrate and fluoride in Kakhk city and its rural areas, Iran. *J. Food Compos. Anal.* **2023**, *115*, 104870. [CrossRef]
38. Aladejana, J.A.; Kalin, R.M.; Sentenac, P.; Hassan, I. Assessing the impact of climate change on groundwater quality of the shallow coastal aquifer of eastern dahomey basin, Southwestern Nigeria. *Water* **2020**, *12*, 224. [CrossRef]
39. Panneerselvam, B.; Paramasivam, S.K.; Karuppannan, S.; Ravichandran, N.; Selvaraj, P. A GIS-based evaluation of hydrochemical characterisation of groundwater in hard rock region, South Tamil Nadu, India. *Arab. J. Geosci.* **2020**, *13*, 1–22. [CrossRef]
40. Machiwal, D.; Cloutier, V.; Güler, C.; Kazakis, N. A review of GIS-integrated statistical techniques for groundwater quality evaluation and protection. *Environ. Earth Sci.* **2018**, *77*, 1–30. [CrossRef]
41. Sebei, A.; Slama, T.; Helali, M.A. Hydrochemical characterization and geospatial analysis of groundwater quality in Cap Bon region, northeastern Tunisia. *Environ. Earth Sci.* **2018**, *77*, 1–18. [CrossRef]
42. Rivett, M.O.; Budimir, L.; Mannix, N.; Miller, A.V.; Addison, M.J.; Moyo, P.; Wanangwa, G.J.; Phiri, O.L.; Songola, C.E.; Nhlema, M.; et al. Responding to salinity in a rural African alluvial valley aquifer system: To boldly go beyond the world of hand-pumped groundwater supply? *Sci. Total Environ.* **2019**, *653*, 1005–1024. [CrossRef]
43. Al-Jawad, J.Y.; Al-Jawad, S.B.; Kalin, R.M. Decision-making challenges of sustainable groundwater strategy under multi-event pressure in arid environments: The Diyala River Basin in Iraq. *Water* **2019**, *11*, 2160. [CrossRef]
44. Mahammad, S.; Islam, A. Evaluating the groundwater quality of Damodar Fan Delta (India) using fuzzy-AHP MCDM technique. *Appl. Water Sci.* **2021**, *11*, 1–17. [CrossRef]

45. Bernard, E.; Ayeni, N. Physicochemical Analysis of Groundwater Samples of Bichi Local Government Area of Kano State of Nigeria. *World Environ.* **2012**, *2*, 116–119. [CrossRef]
46. Hamidu, H.; Halilu, F.B.; Yerima, K.M.; Garba, L.M.; Suleiman, A.A.; Kankara, A.I.; Abdullahi, I.M. Heavy metals pollution indexing, geospatial and statistical approaches of groundwater within Challawa and Sharada industrial areas, Kano City, North-Western Nigeria. *SN Appl. Sci.* **2021**, *3*, 690. [CrossRef]
47. Suleiman, A.; Ibrahim, A.; Abdullahi, U. Statistical Explanatory Assessment of Groundwater Quality in Gwale LGA, Kano State, Northwest Nigeria. *Hydrospatial Anal.* **2020**, *4*, 1–13. [CrossRef]
48. Usman, F.U.; Aliyu, B. Impact of Pit Latrine on groundwater quality in some communities of Nguru town, Nguru Local Government area, Yobe State, Nigeria. *East African Sch. Multidiscip. Bull.* **2020**, *3*, 218–225. [CrossRef]
49. Waziri, M.; Ogugbuaja, V.O. Interrelationships between physicochemical water pollution indicators: A case study of River Yobe-Nigeria. *Am. Jouran Sci. Ind. Res.* **2010**, *1*, 76–80.
50. Adeyeri, O.E.; Lawin, A.E.; Laux, P.; Ishola, K.A.; Ige, S.O. Analysis of climate extreme indices over the Komadugu-Yobe basin, Lake Chad region: Past and future occurrences. *Weather Clim. Extrem.* **2019**, *23*, n100194. [CrossRef]
51. Goes, B.J.M. Effects of river regulation on aquatic macrophyte growth and floods in the Hadejia-Nguru wetlands and flow in the Yobe River, northern Nigeria; implications for future water management. *River Res. Appl.* **2002**, *18*, 81–95. [CrossRef]
52. Ahmed, S.D.; Agodzo, S.K.; Adjei, K.A.; Deinmodei, M.; Ameso, V.C. Preliminary investigation of flooding problems and the occurrence of kidney disease around Hadejia-Nguru wetlands, Nigeria and the need for an ecohydrology solution. *Ecohydrol. Hydrobiol.* **2018**, *18*, 212–224. [CrossRef]
53. Adeyeri, O.E.; Laux, P.; Lawin, A.E.; Ige, S.O.; Kunstmann, H. Analysis of hydrometeorological variables over the transboundary komadugu-yobe basin, West Africa. *J. Water Clim. Chang.* **2020**, *11*, 1339–1354. [CrossRef]
54. Avbovbo, A.A.; Ayoola, F.O.; Osahon, G.A. Depositional and Structural Styles in Chad Basin of Northeastern Nigeria. *Am. Assoc. Pet. Geol. Bull.* **1986**, *70*, 1787–1798. [CrossRef]
55. McCurry, P. Pan-african orogeny in northern Nigeria. *Bull. Geol. Soc. Am.* **1971**, *82*, 3251–3262. [CrossRef]
56. Obaje, N.G.; Wehner, H.; Hamza, H.; Scheeder, G. New geochemical data from the Nigerian sector of the Chad basin: Implications on hydrocarbon prospectivity. *J. African Earth Sci.* **2004**, *38*, 477–487. [CrossRef]
57. Obaje, N.G. *Geology and Mineral Resources of Nigeria*; Springer: Berlin/Heidelberg, Germany, 2011; Volume 131.
58. Lopez, T.; Antoine, R.; Kerr, Y.; Darrozes, J.; Rabinowicz, M.; Ramillien, G.; Cazenave, A.; Genthon, P. *Subsurface Hydrology of the Lake Chad Basin from Convection Modelling and Observations*; Springer: Amsterdam, The Netherlands, 2016; Volume 37. [CrossRef]
59. Bura, B.; Goni, I.B.; Sheriff, B.M.; Gazali, A.K. Occurrence and distribution of fluoride in groundwater of chad formation aquifers in Borno state, Nigeria. *Int. J. Hydrol.* **2018**, *2*, 528–537. [CrossRef]
60. Ola-Buraimo, A.O.; Abdulganiyu, Y. Palynology and stratigraphy of the Upper Miocene Chad Formation, Bornu Basin, northeastern Nigeria. *J. Palaeogeogr.* **2017**, *6*, 108–116. [CrossRef]
61. Adegoke, O.S.; Agumanu, A.E.; Benkhelil, M.J.; Ajayi, P.O. New stratigraphic, sedimentologic and structural data on the kerri-kerri formation, Bauchi and Borno States, Nigeria. *J. African Earth Sci.* **1986**, *5*, 249–277. [CrossRef]
62. Wali, S.U.; Alias, N.; Harun, S.B. Quality reassessment using water quality indices and hydrochemistry of groundwater from the Basement Complex section of Kaduna Basin, NW Nigeria. *SN Appl. Sci.* **2020**, *2*, 1–21. [CrossRef]
63. Vassolo, S.; Daïra, D. *Lake Chad: Sustainable Water Managemen*; Report No. 4; BGR: Berlin, Germany, 2012.
64. Edmunds, W.M.; Fellman, E.; Goni, I.B.; Prudhomme, C. Spatial and temporal distribution of groundwater recharge in northern Nigeria. *Hydrogeol. J.* **2002**, *10*, 205–215. [CrossRef]
65. Edmunds, W.M.; Fellman, E.; Goni, I.B. Lakes, groundwater and palaeohydrology in the Sahel of NE Nigeria: Evidence from hydrogeochemistry. *J. Geol. Soc. London.* **1999**, *156*, 345–355. [CrossRef]
66. Akujieze, C.N.; Coker, S.J.L.; Oteze, G.E. Groundwater in Nigeria—A millennium experience—Distribution, practice, problems and solutions. *Hydrogeol. J.* **2003**, *11*, 259–274. [CrossRef]
67. Edet, A.E.A.; Nganje, T.N.; Ukpong, A.J. Groundwater chemistry and quality of Nigeria: A status review. *Afr. J. Environ. Sci. Technol.* **2012**, *5*, 1152–1169. [CrossRef]
68. Le Coz, M.; Genthon, P.; Adler, P.M. Multiple-Point Statistics for Modeling Facies Heterogeneities in a Porous Medium: The Komadugu-Yobe Alluvium, Lake Chad Basin. *Math. Geosci.* **2011**, *43*, 861–878. [CrossRef]
69. Carter, R.C.; Alkali, A.G. Shallow groundwater in the northeast arid zone of Nigeria. *Q. J. Eng. Geol.* **1996**, *29*, 341–355. [CrossRef]
70. APHA; AWWA; WEF. *Standard Methods for Examination of Water and Wastewater*, 22nd ed.; American Public Health Association: Washington, DC, USA, 2012; p. 1360. ISBN 978-087553-013-0. Available online: http://www.standardmethods.org/ (accessed on 14 February 2024).
71. Adimalla, N.; Venkatayogi, S. Geochemical characterization and evaluation of groundwater suitability for domestic and agricultural utility in semi-arid region of Basara, Telangana State, South India. *Appl. Water Sci.* **2018**, *8*, 1–14. [CrossRef]
72. WHO. A Global Overview of National Regulations and Standards for Drinking-Water Quality. 2018. Available online: http://apps.who.int/bookorders (accessed on 14 February 2024).
73. Eyankware, M.O.; Aleke, C.G.; Selemo, A.O.I.; Nnabo, P.N. Hydrogeochemical studies and suitability assessment of groundwater quality for irrigation at Warri and environs. Niger delta basin, Nigeria. *Groundw. Sustain. Dev.* **2020**, *10*, 100293. [CrossRef]
74. White, A.F.; Schulz, M.S.; Lowenstern, J.B.; Vivit, D.V.; Bullen, T.D. The ubiquitous nature of accessory calcite in granitoid rocks: Implications for weathering, solute evolution, and petrogenesis. *Geochim. Cosmochim. Acta* **2005**, *69*. [CrossRef]

75. Davis, R.J.M.; DeWiest, S.N. *Hydrogeology*; Wiley: New York, NY, USA, 1966.
76. Sawyer, P.; McCarthy, C. *Chemistry for Environmental Engineering and Science*, 2nd ed.; McGraw-Hill: New York, NY, USA, 1967.
77. Bloise, A.; Critelli, T.; Catalano, M.; Apollaro, C.; Miriello, D.; Croce, A.; Barrese, E.; Liberi, F.; Piluso, E.; Rinaudo, C.; et al. Asbestos and other fibrous minerals contained in the serpentinites of the Gimigliano-Mount Reventino Unit (Calabria, S-Italy). *Environ. Earth Sci.* **2014**, *71*, 3773–3786. [CrossRef]
78. Uddin, M.G.; Diganta, M.T.; Sajib, A.M.; Hasan, M.A.; Moniruzzaman, M.; Rahman, A.; Olbert, A.I.; Moniruzzaman, M. Assessment of hydrogeochemistry in groundwater using water quality index model and indices approaches. *Heliyon* **2023**, *9*, e19668. [CrossRef]
79. Vaughan, D.J. Sulfide mineralogy and geochemistry: Introduction and overview. *Rev. Mineral. Geochemistry* **2006**, *61*, 1–5. [CrossRef]
80. Akpata, E.S.; Danfillo, I.S.; Otoh, E.C.; Mafeni, J.O. Geographical mapping of fluoride levels in drinking water sources in Nigeria. *Afr. Health Sci.* **2009**, *9*, 227–233.
81. Giwa, A.S.; Memon, A.G.; Ahmad, J.; Ismail, T.; Abbasi, S.A.; Kamran, K.; Wang, B.; Segun, B.; Seydou, H. Assessment of high fluoride in water sources and endemic fluorosis in the North-Eastern communities of Gombe State, Nigeria. *Environ. Pollut. Bioavailab.* **2021**, *33*, 31–40. [CrossRef]
82. Malago, N.N.M.; Edikafubeni, J.; Alfred, M. Fluoride Levels in Surface and Groundwater in Africa: A Review. *Am. J. Water Sci. Eng.* **2017**, *3*, 1. [CrossRef]
83. Waziri, M.; Musa, U.; Hati, S.S. Assessment of Fluoride Concentrations in Surface Waters and Groundwater Sources in Northeastern Nigeria. *Resour. Environ.* **2012**, *2*, 67–72. [CrossRef]
84. Haritash, A.K.; Aggarwal, A.; Soni, J.; Sharma, K.; Sapra, M.; Singh, B. Assessment of fluoride in groundwater and urine, and prevalence of fluorosis among school children in Haryana, India. *Appl. Water Sci.* **2018**, *8*, 1–8. [CrossRef]
85. Yadav, J.P.; Lata, S.; Kataria, S.K.; Kumar, S. Fluoride distribution in groundwater and survey of dental fluorosis among school children in the villages of the Jhajjar District of Haryana, India. *Environ. Geochem. Health* **2009**, *31*, 431–438. [CrossRef]
86. Gibbs, J.R. Mechanisms Controlling World Water Chemistry. *Science* **1970**, *170*, 1088–1090. [CrossRef]
87. Marandi, A.; Shand, P. Groundwater chemistry and the Gibbs Diagram. *Appl. Geochem.* **2018**, *97*, 209–212. [CrossRef]
88. Adimalla, N.; Vasa, S.K.; Li, P. Evaluation of groundwater quality, Peddavagu in Central Telangana (PCT), South India: An insight of controlling factors of fluoride enrichment. *Model. Earth Syst. Environ.* **2018**, *4*, 841–852. [CrossRef]